Available online at www.sciencedirect.com
SCIENCE DIRECT®
Journal of Power Sources 152 (2005) 233–244
JOURNAL OF POWER SOURCES
www.elsevier.com/locate/jpowsour

Fuel economy of hybrid fuel-cell vehicles☆

Rajesh K. Ahluwalia*, X. Wang, A. Rousseau

Argonne National Laboratory, 9700 South Cass Avenue, Argonne, IL 60439, USA

Received 6 December 2004; accepted 10 January 2005
Available online 3 May 2005

Abstract

The potential improvement in fuel economy of a mid-size fuel-cell vehicle by combining it with an energy storage system has been assessed. An energy management strategy is developed and used to operate the direct hydrogen, pressurized fuel-cell system in a load-following mode and the energy storage system in a charge-sustaining mode. The strategy places highest priority on maintaining the energy storage system in a state where it can supply unanticipated boost power when the fuel-cell system alone cannot meet the power demand. It is found that downsizing a fuel-cell system decreases its efficiency on a drive cycle which is compensated by partial regenerative capture of braking energy. On a highway cycle with limited braking energy the increase in fuel economy with hybridization is small but on the stop-and-go urban cycle the fuel economy can improve by 27%. On the combined highway and urban drive cycles the fuel economy of the fuel-cell vehicle is estimated to increase by up to 15% by hybridizing it with an energy storage system.

Keywords: Fuel economy; Hydrogen fuel cell; Hybrid vehicles

1. Introduction

Automobile manufacturers are introducing gas-electric hybrids to overcome the drop off in the efficiency of the internal combustion engines (ICEs) at part loads. Hybrid electric vehicles (HEVs) use a small ICE together with a battery-powered motor to boost acceleration power. The smaller engine of the HEV gives better fuel economy than the ICE in a conventional vehicle because it is operated closer to the rated power where it is efficient. The battery and electric motor provide traction power at low loads, where the energy conversion efficiency would be poor for the ICE. Energy from braking the vehicle, which is dissipated as heat in the conventional mechanical braking systems, is charged into the HEV battery for reuse. According to different studies, hybridization has the potential to reduce the fuel consumption of gasoline ICE vehicles by 20–30% on standard drive cycles [1–3].

In contrast to the conventional ICE, fuel-cell systems (FCS) have the characteristic that the efficiency does not degrade at part load and in fact can be much higher. This is particularly advantageous in transportation applications because the vehicles are mostly operated at part load conditions; the average demand on standard U.S. drive cycles on which the fuel economy is measured is less than 20% of the rated power of the engine. A recent study concluded that the fuel economy of hydrogen fuel-cell electric vehicles (FCEVs) can be 2.5–3 times the fuel economy of the conventional gasoline ICE vehicles [4].

Because the fuel cells are more efficient at part load than at rated power, the case for hybridizing a fuel-cell vehicle is different. One motivation for hybridizing the FC vehicle is to improve its fuel economy by recovering a portion of the braking energy. Hybridization can also help if the energy storage device has higher specific power ($kWe\,kg^{-1}$) and lower cost ($\$\,kWe^{-1}$) than the FCS so that the hybrid system is lighter and less expensive. Because of higher part-load efficiency, even in a hybrid configuration it appears advantageous to preferentially operate the FCS in a load-following mode and to use the power from the battery when the FCS alone cannot meet the power demand.

The purpose of this study is to assess the potential improvement in fuel economy of a FCEV by hybridizing it with an energy storage system (ESS). The study is based on a mid-

☆ This paper was presented at the 2004 Fuel Cell Seminar, San Antonio, TX, USA.

* Corresponding author. Tel.: +1 630 252 5979; fax: +1 630 252 5287.
E-mail address: walia@anl.gov (R.K. Ahluwalia).

0378-7753/$ – see front matter © 2005 Published by Elsevier B.V.
doi:10.1016/j.jpowsour.2005.01.052

Table 1
Vehicle specifications and traction power requirements

Reference ICE vehicle specifications		FCEV traction power requirements	
Gross vehicle weight	1695 kg	Gross vehicle weight	1950 kg
Frontal area	2.2 m^2	Z-60 (10 s)	120 kWe
Drag coefficient	0.32	Top speed (100 mph)	65 kWe
Coefficient of rolling friction	0.009	55 mph at 6.5% grade	62 kWe

size family sedan as the vehicle platform, a direct-hydrogen pressurized FCS as the energy converter and a lithium-ion battery pack as the ESS. The results are presented for different drive cycles as a function of the degree of hybridization (DOH) defined as the ratio of the electric power that can be delivered by the ESS to the total power that can be delivered by the ESS and the FCS. In comparing the fuel economies of fuel-cell hybrid electric vehicles (FCHEVs) with different DOH we require that they have the same acceleration performance by holding the combined rated power of the FCS and ESS as constant. Consequently, the FCS is downsized as the DOH is increased by making the ESS larger.

For ease of comprehension the fuel economy of hydrogen fuel-cell vehicle is quoted in this paper on the basis of miles per gallon gasoline equivalent (mpgge): 1 kg of hydrogen is approximately equivalent to 1 gal of gasoline in lower heating value (LHV). We quantify the potential gain in fuel economy in terms of a multiplier defined as the ratio of mpgge achieved by the FCEV to the mpg achieved by the reference gasoline ICEV on the same platform. Some results are in the form of tank-to-wheel (TTW) efficiency defined as the mechanical energy available at the wheels of the vehicle divided by the LHV of hydrogen supplied to the FCS. The TTW efficiency is a measure of the performance of the FCS and the electric drive train and depends on the drive cycle as well.

2. Vehicle and fuel-cell system

A mid-size family sedan was selected as the reference ICE vehicle platform for which Table 1 lists the major parameters that affect its fuel economy, including mass, drag coefficient, frontal area and coefficient of rolling friction.

Fig. 1 shows the schematic of the direct-hydrogen pressurized FCS used as the energy converter. At the rated power point, the polymer electrolyte fuel cell (PEFC) stack operates at 2.5 atm and 80 °C to yield an overall system efficiency of 50% (based on lower heating value of hydrogen). Compressed hydrogen and air are humidified to 90% relative humidity (RH) at the stack temperature using process water and heat from the stack coolant. The system pressure is lower than 2.5 atm at part load and is determined by the operating map of the compressor-expander module (CEM) [5]. The nominal flow rate of cathode air is two times what is needed for complete oxidation of hydrogen (50% oxygen utilization). Process water is recovered from spent air in an inertial separator just downstream of the stack, in a condenser and in a demister at the turbine exhaust. The waste heat transferred to the coolant in the stack is either used for humidifying the anode and cathode streams or rejected in a radiator.

Our interest is in a charge-sustaining hybrid fuel-cell vehicle in which the FCS is operated in a load-following mode. In this type of a hybrid system, FCS provides the traction power under normal driving conditions with the ESS supplying boost power under transient conditions. ESS also stores part of the energy that must otherwise be dissipated when the vehicle brakes. The manner in which the energy stored in ESS from regenerative braking is discharged and used for traction is determined by the vehicular energy management strategy. To be competitive with the conventional ICE propulsion system in terms of drivability and performance, the FCS in this type of a hybrid vehicle must satisfy the following requirements:

(a) FCS alone must be capable of meeting the vehicle power demands under all sustained driving conditions. These include a specified top sustained speed, taken as 100 mph (mile h^{-1}) in this study, and ability to maintain the vehicle at 55 mph speed at 6.5% grade for 20 min.
(b) With the assistance of ESS, the FCS must have the response time to allow the vehicle to accelerate from 0 to 60 mph (Z-60) in a specified time, taken as 10 s in this study.
(c) FCS must have 1 s transient response time for 10–90% power.
(d) FCS must reach maximum power in 15 s for cold start from 20 °C ambient temperature and in 30 s from −20 °C ambient temperature.

We used the following approach in selecting FCS parameters to meet the above requirements:

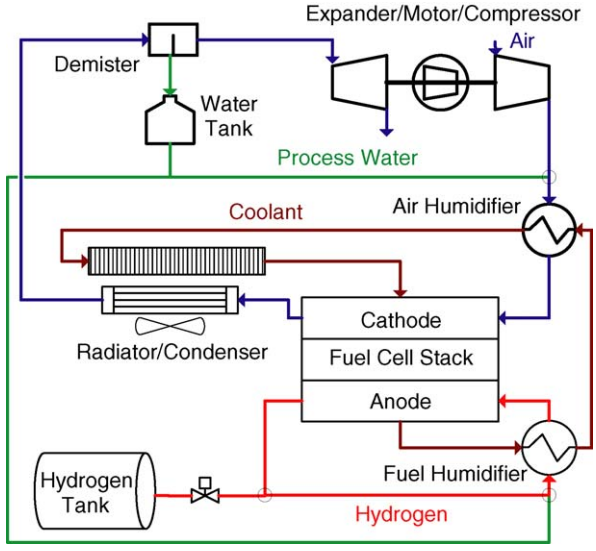

Fig. 1. Schematic of direct-hydrogen pressurized FCS.

(a) We define the minimum power rating of the FCS to be the higher of the power demand at 100 mph sustained speed and the power needed at 55 mph at 6.5% grade.
(b) We further require that the FCS be 50% efficient at the rated power point. This requirement determines the cell voltage at rated power.
(c) We size the heat rejection system by requiring that the FCS be able to operate without overheating at ambient temperatures up to 42 °C.
(d) We size the water management system so that the FCS is water balanced for all sustained loads at 50% oxidant utilization and ambient temperatures up to 42 °C.
(e) We meet the 1 s transient time target by overloading the CEM electric motor for short time periods.

We iterated between the FCS and vehicle parameters to determine that 120 kWe FCS peak power is needed to accelerate the FCEV (1950 kg gross vehicle weight including 136-kg payload) from 0 to 60 mph in 10 s and that 65 kWe is needed to maintain the vehicle at 100 mph top sustained speed. Also, the vehicle needs 62 kWe FCS power at the gradeability condition, 55 mph at 6.5% grade with 600-kg payload. Accordingly, we consider fuel-cell systems with 65–120 kWe rated power. The 65 kWe FCS needs the largest ESS (55 kWe) whereas the 120 kWe FCS can power the vehicle without an ESS.

Computer codes GCtool and PSAT [6,7] were employed to determine the characteristics of four mid-size vehicles that use FCS with 65, 80, 100 and 120 kWe rated power and these are summarized in Table 2. In listing the estimated weights, the hydrogen storage medium has been included with the FCS and the ESS with the electric drive train. It is assumed that hydrogen is stored as compressed gas at 5000 psi and in sufficient quantity for 320-mile driving range. Note that the gross vehicle weight rating for the FCEV is 225 kg more than for the ICEV and about the same as for the FCHEV with 65 kWe FCS and 55 kWe (peak pulse discharge power) ESS.

2.1. Electric drive train

Fig. 2 shows the configuration of the electric drive train considered in this study. The input voltage of the inverter for the ac traction motor floats with the output voltage of the PEFC stack. A bi-directional dc/dc converter is used to step-up the ESS voltage to match the PEFC stack voltage during discharge or to step-down the inverter/rectifier output voltage to the appropriate level for charging the battery during regenerative braking. The dc/dc converter is assumed to have an average efficiency of 95% in the step-up and step-down modes.

The mechanical energy at the motor shaft is transmitted to the wheels via a one-speed reduction gear (94% peak efficiency) and a final drive (differential with specified gear ratio, 93% peak efficiency). A parametric study was performed to determine the optimum gear ratio and the motor power needed to obtain 100 mph top speed and be able to accelerate from 0 to 60 mph in 10 s. The study revealed that the top speed and acceleration criteria can be met with a motor that provides 110 kW peak and 65 kW continuous shaft power (0.66 m wheel diameter). Fig. 3 is a map that we have constructed for a 110 kW/65 kW peak/continuous-power motor from the data obtained in our laboratory for a combined inverter and a brushless permanent magnet motor of similar capacity [8]. The map is used in our simulations to estimate the traction inverter motor (TIM) efficiency as a function of motor torque and rotating speed. Applied to our FCEV platform, the TIM has a peak efficiency of 94% at 75 mph vehicle speed which drops to 84–85% as the speed is raised to 100 mph or lowered to 10 mph [5].

2.2. Energy storage system

In our simulations, we have used a Li-ion battery pack, tested in our laboratory, as the ESS, each cell of which has a rated C_5 capacity of 6 Ah with 2.9–4.0 V safe (continuous) operating voltage range. Based on our test data, the cell voltage can be raised to 4.1 V or lowered to 2.5 V for brief 5 s bursts. The maximum allowable discharge current is 250 A for state of charge (SOC) above 0.2 and is assumed to linearly decreases to 0 over the SOC range 0.2–0. The maximum allowable regenerative current is 200 A for SOC < 0.7 and is assumed to decrease to 0 over the SOC range 0.7–1. We determine the number of cells in the ESS and the minimum SOC to deliver peak pulse discharge power of 20, 40 or 55 kWe for 10 s and to have specified available (C_1) energy over the range SOC_{min} to the target SOC. In sizing the ESS, we fix the ratio of the available energy to the pulse discharge power as 12 Wh kW^{-1} (e.g., 300 Wh available energy for 25 kW pulse discharge power).

2.3. Performance of fuel-cell systems

The computer code GCtool [6] was used to analyze the performance of the fuel-cell systems. Fig. 4 presents the modeled steady-state efficiency as a function of the net power produced by the FCS. At the idling condition the PEFC stack produces just enough power to operate the CEM. The idling point is determined by the maximum turn-down (defined as the ratio of air flow rate at rated power to the minimum flow discharged by the compressor, 20 in this study) of the CEM. At the idling condition the FCS consumes about 0.1% of the hydrogen flow rate at rated power if the maximum turn-down of the CEM is 20.

Fig. 4 shows that even though each system has the same efficiency at rated power, at given load, the FCS with higher rated power generally has higher efficiency. For the FCS configuration analyzed, the PEFC stack cannot be maintained at 80 °C at low loads where it operates at close to the ambient pressure and the waste heat transferred to the coolant in the stack is insufficient to humidify the feed streams to 90% RH. Also, the cell voltage is 880 mV at the idling condition

Table 2
Hybrid FCEV platforms for mid-size sedan

	Gasoline ICE	FCEV 120 kWe	FCHEV-1 100 kWe	FCHEV-2 80 kWe	FCHEV-3 65 kWe
Power					
IC engine/fuel-cell system (kW)	114	120	100	80	65
Electric motor (peak/continuous) (kW)		110/65	110/65	110/65	110/65
Energy storage system (peak) (kWe)			20	40	55
Transmission type	5 Spd	1 Spd	1 Spd	1 Spd	1 Spd
Weights					
Glider (body and chassis) + payload (kg)	1165	1215	1215	1215	1215
ICE/fuel-cell system (kg)	310	380	345	310	280
Drive train (kg)	220	325	375	400	410
Gross vehicle weight (kg)	1695	1920	1945	1930	1920
Accessory power					
Mechanical (W)	700	0	0	0	0
Electrical (We)	500	500	500	500	500
Simulation results – performance[a]					
Top speed (mph)	>115	100	100	100	100
0–60 mph (s)	10.5	9.7	9.7	9.6	9.5
0–30 mph (s)		3.6	3.6	3.4	3.4
50–80 mph (s)		10.4	10.5	10.5	10.5
Maximum vehicle acceleration ($m\,s^{-2}$)		4.2	4.2	4.3	4.3
6.5% at 55 mph (%)	Yes	Yes	Yes	Yes	Yes

[a] Initial SOC = 0.65.

(somewhat less than the open-circuit voltage at 1 atm) and drops slowly to 690 mV at the rated power point.

Fig. 5 indicates that the performance of the FCS on a drive cycle can deviate significantly from its steady-state behavior. The dynamic efficiency is not a monotonic function of power demand and can be higher than the steady-state efficiency during periods of deceleration and lower than the steady-state efficiency when the vehicle accelerates [4,5].

2.4. Drive cycles

We have analyzed the fuel economy of hybrid vehicles over five different drive cycles. Federal Highway Drive Schedule (FHDS) and Federal Urban Drive Schedules (FUDS) are the drive cycles used by U.S. EPA to certify that light duty vehicles meet the federal emissions and fuel economy standards. FHDS represents highway and rural driving at speeds up to 60 mph with a warmed-up engine. FUDS simulates stop-and-go urban driving with engine started from 20 to 30 °C ambient temperature. US06 is another cycle used for emission certification of light duty vehicles in the U.S. It incorporates aggressive, high speed and high acceleration driving behavior, rapid speed fluctuations, and start-up after overnight parking. The standard cycle used in Europe for emission certification and comparison of the fuel economy of light duty vehicles is NEDC, the New European Drive Cycle. It simulates both the city (50 $km\,h^{-1}$ top speed, 19 $km\,h^{-1}$ average speed, 780 s duration, cold start)

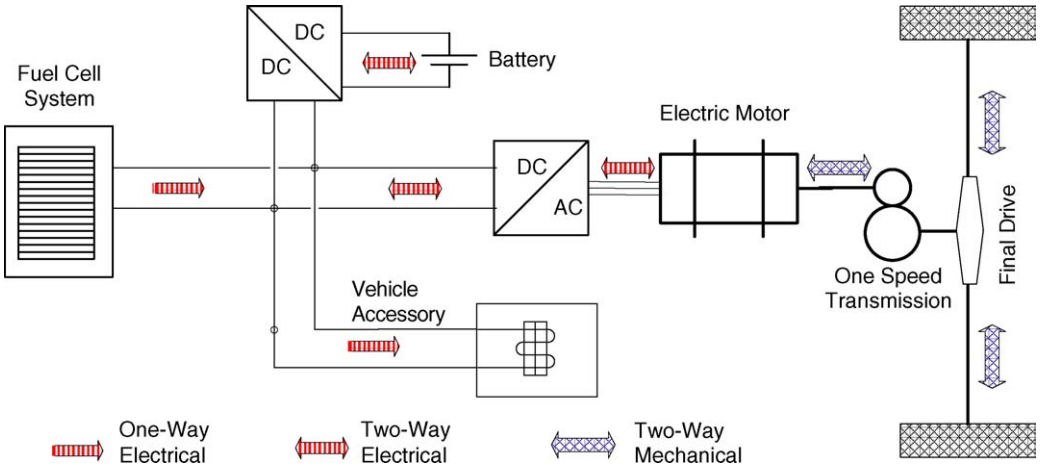

Fig. 2. Schematic of electric drive train for FCHEV.

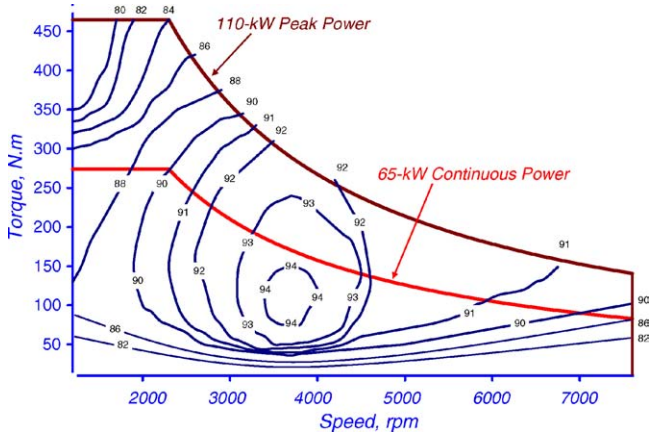

Fig. 3. Combined efficiency of inverter and permanent magnet motor.

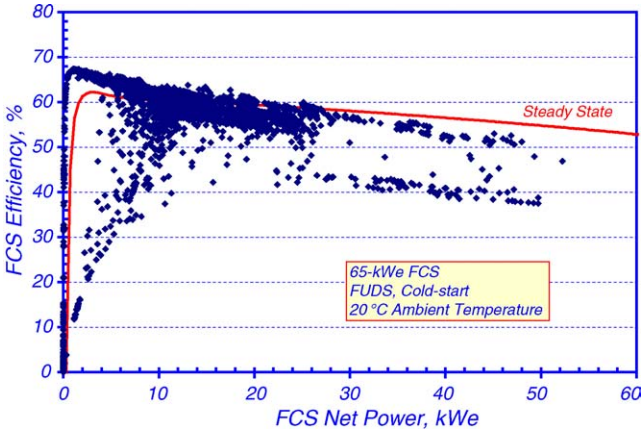

Fig. 5. Dynamic FCS performance.

and highway (120 km h^{-1} top speed, 62.6 km h^{-1} average speed, 400 s duration, warm start) driving conditions. Similarly, J1015 is the drive cycle used in Japan for emission certification and comparative measurement of fuel economy of light duty vehicles.

Table 3 summarizes the drive cycles in terms of the duration, distance traveled and average speed. For each cycle, we have used the computer code PSAT to estimate the traction energy requirement and the fraction of the traction energy that is involved in braking for the stand-alone FCEV platform with vehicle parameters listed in Tables 1 and 2. For later reference these are included in Table 3.

2.5. Energy management

A hierarchical set of priorities is used to regulate the flow of power into and out of the energy storage system. The highest priority is placed on maintaining the ESS near its target state of charge so that it can provide assist power in transients when the FCS is unable to meet the vehicle power demand. The next level of priority is to maintain the ESS in a position (i.e., lowest SOC) that maximizes its ability to accept regenerative braking energy when it becomes available. In order to accommodate the two conflicting priorities, our strategy is to attempt to discharge the ESS immediately after a regenerative braking event that raises the SOC above the target value (0.65 in this work). During this time the priority is given on drawing the maximum power from the ESS with the FCS providing the balance to meet the vehicle power demand. The maximum power draw from ESS is a function of the battery SOC but is always less than the instantaneous power demand.

Fig. 6 has been constructed to illustrate our energy management strategy. It presents the maximum pulse power (calculated from a battery model formulated on the basis of the hybrid-pulse power characterization testing of a battery pack) that can be discharged from a single cell of the Li-ion battery if the FCS is unable to meet the instantaneous power demand. Within the envelope of allowed SOC, the pulse discharge power varies between 575 and 650 W cell^{-1}. Fig. 6 also presents the maximum pulse power (calculated from the battery model) that a single cell can accept from regenerative braking. The pulse charge power varies from 350 W cell^{-1} at the target SOC (0.65) to 500 W cell^{-1} at the lower limit of SOC (0.3). Included in Fig. 6 is the modeled power that

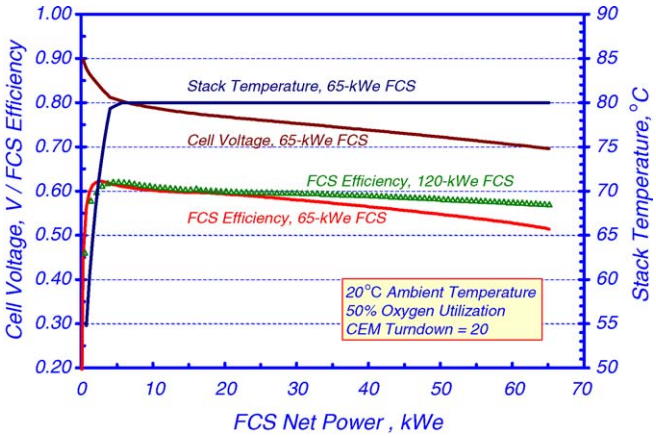

Fig. 4. Steady-state FCS performance.

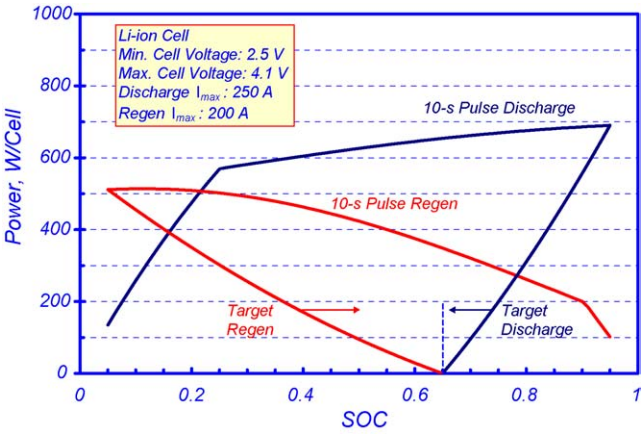

Fig. 6. Battery power management strategy.

Table 3
Summary of drive cycles simulated in this study

Schedule	FUDS	FHDS	US06	J1015	NEDC
Distance (km)	11.8	16.4	12.8	4.2	11.0
Duration (s)	1372	740	596	660	1180
Average speed (km h^{-1})	32	78	77	23	34
Maximum speed (km h^{-1})	90	95	130	70	120
Number of stops	23	1	8	7	13
Idle time (%)	18	0	7	32	25
Start-up	Cold	Warm	Cold	Warm	Cold
Traction energy (Wh)	1700	2050	2655	575	1520
Braking energy (% of traction energy)	50	13	34	53	35

is drawn from the FCS to charge a single cell of the Li-ion battery if the SOC drops below the target value of 0.65. The modeled charge power is less than the maximum pulse regenerative power and goes to zero as the SOC approaches the target value. Also included in Fig. 6 is the modeled power that is discharged from a single cell of the battery if the SOC exceeds the target value. The modeled discharge power is less than the maximum pulse discharge power and goes to zero as the SOC approaches the target value; the actual discharge power may be further limited by the instantaneous traction power demand.

Fig. 7 is an example of the implementation of the above power management strategy in a segment of FUDS simulation. It shows periods (610–620 and 667–680 s) during which the ESS is charged by regenerative braking, period (645–648 s) during which the ESS is the main source of traction power with FCS providing the assist, and the period (648–668 s) in which FCS is the primary power source and the ESS is discharged to reach the target SOC. It also includes a short period of time (~652 s) in which the ESS supplies power boost to meet the sudden surge in power demand.

2.6. Simulation methodology

The vehicle analysis code PSAT and the fuel-cell system analysis code GCtool were tightly integrated to conduct full dynamic simulations of the fuel-cell vehicles on the prescribed drive cycles and performance cycles. The choice of vehicle parameters was first validated by comparing the simulated fuel economy of the reference gasoline ICEV with the published values of 29 mpg on FHDS and 20 mpg on FUDS. The simulated fuel economy was slightly higher than the published value for FUDS because the effect of cold start is not reflected in the ICE map used in PSAT. The GCtool model, however, does account for cold start of fuel-cell systems.

Special care was taken in determining the fuel economy of hybrid vehicles on a consistent and reproducible basis by running simulations such that there was no net transfer of energy into or out of the energy storage system. This involved determining the initial battery SOC so that the SOC at the end of the drive cycle was the same as at the start of the cycle.

3. Fuel economy

Fig. 8 compares the simulated fuel economy of FCEV with the fuel economy of ICEV on the highway and urban schedules. In order to reflect the real world driving experience, EPA adjusts the fuel economy of ICEVs measured in laboratory tests by a factor of 0.78 for the highway schedule and 0.9 for the urban schedule. We apply the same correction

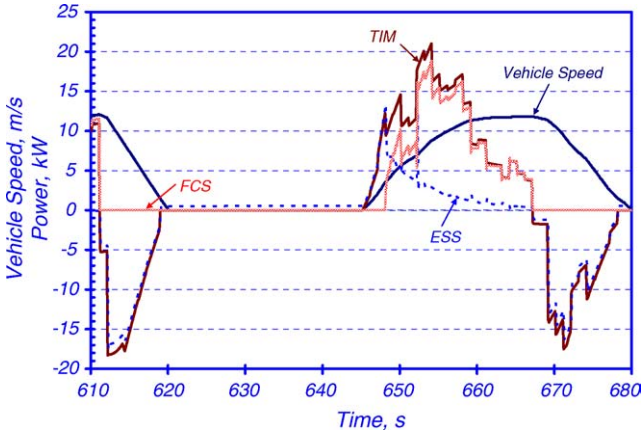

Fig. 7. Example implementation of energy management strategy.

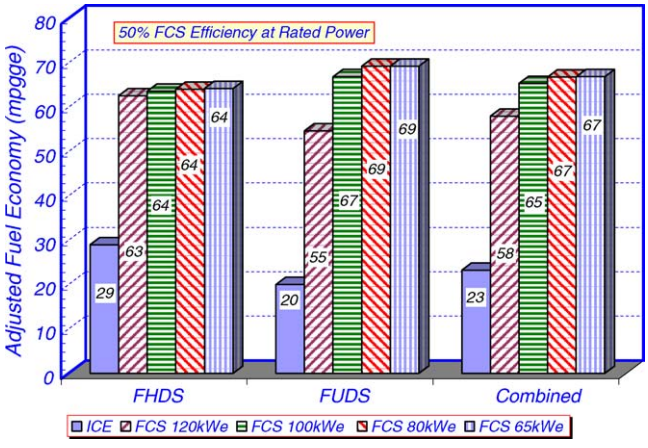

Fig. 8. Effect of hybridization on fuel economy of FCEV.

factors to our simulation results for the FCEV. Also, as is done for ICEV, we define the combined fuel economy (FE) over urban and highway schedules as the following weighted average.

$$\mathrm{FE}_{\mathrm{combined}} = \frac{1}{0.55/\mathrm{FE}_{\mathrm{FUDS}} + 0.45/\mathrm{FE}_{\mathrm{FHDS}}} \quad (1)$$

On the highway schedule, the simulated fuel economy of the stand-alone FCEV after adjustment is 63 mpgge compared to 29 mpgge for the ICEV. On FHDS, hybridization is seen to have a small effect (<3% improvement) on the fuel economy of the fuel-cell vehicle.

On the urban schedule, the simulated fuel economy of the stand-alone FCEV after adjustment is 55 mpgge compared to 20 mpgge for the ICEV. The fuel economy of FCEV improves to 67 mpgge with a small ESS (20 kWe) and to 69 mpgge with a larger ESS (40 kWe). Further increase in the size of the ESS to 55 kWe results in a marginal improvement in the fuel economy. Note that whereas the fuel economy of the stand-alone FCEV (and ICEV) is lower on the urban schedule than on the highway schedule, the fuel economy of the FCHEV can be higher on the urban schedule than on the highway schedule.

On the combined highway and urban schedules, the simulated fuel economy of the stand-alone FCEV is 2.5 times the fuel economy of the ICEV. With hybridization, the fuel economy multiplier for the combined schedules increases by about 15% to 2.9 times. The multiplier increases by about 3% on the highway portion and by about 27% on the urban portion of the combined cycle.

Fig. 9 presents the effect of DOH on FCS efficiency, recoverable braking energy, recovered braking energy and the TTW efficiency for the highway and urban schedules. On FHDS, the cumulative efficiency of the FCS (defined as the fraction of the LHV of hydrogen consumed on a drive cycle that is converted to electric energy by the FCS) is seen to decrease from 62% to 60% as the FCS is downsized from 120 to 65 kWe. This decrease in cumulative FCS efficiency is offset by the recovery of braking energy. Our simulations indicate that with a 20 kWe ESS, 67% of the braking energy on FHDS is recoverable at the wheels, 21% of which is lost in the electric drive train so that 53% is actually recovered to recharge the battery. With a 55 kWe ESS, 95% of the braking energy is recoverable at the wheels and 70% is available for recharging the battery. On FHDS, braking involves only 13% of the traction energy so that increase in recovered braking energy with increase in ESS size marginally compensates for the corresponding decrease in cumulative FCS efficiency with the downsizing of the FCS. The result is that on FHDS the TTW efficiency of FCEV improves by only 3.5% with hybridization.

On FUDS, Fig. 9 shows that the cumulative FCS efficiency decreases from 61% to 58% as the FCS is downsized from 120 to 65 kWe. With downsizing of the FCS, the recoverable fraction of the braking energy at the wheels increases from 79% with the 20 kWe ESS to 99% with the 55 kWe ESS and

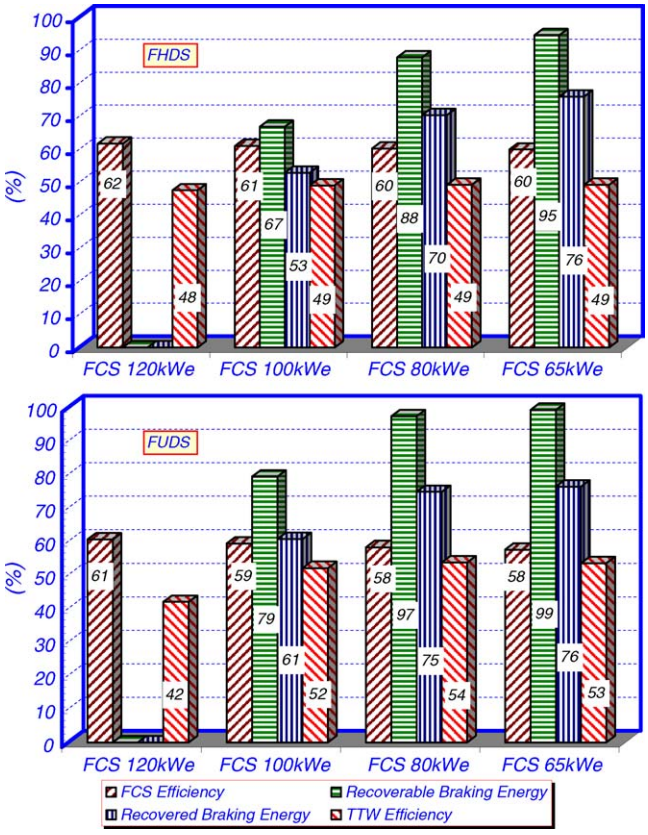

Fig. 9. Effect of hybridization on TTW efficiency on FHDS and FUDS.

the fraction recovered to recharge the battery increases from 61% to 76%. On FUDS, braking involves nearly 50% of the traction energy so that increase in recovered braking energy with increase in ESS size more than compensates for the corresponding decrease in cumulative FCS efficiency with the downsizing of the FCS. The result is that the TTW efficiency on FUDS increases significantly with DOH: the TTW efficiency for the 65 kWe FCS and 55 kWe ESS is about 27% higher than for the stand-alone 120 kWe FCS.

Fig. 10 maps the flow of energy through the various components of the FCEV and FCHEV for the urban schedule. For the stand-alone FCEV, the tank-to-wheel efficiency (η_{TTW}) is given by the following product:

$$\eta_{\mathrm{TTW}} = \eta_{\mathrm{FCS}}\eta_{\mathrm{DT}}(1 - \xi_{\mathrm{acc}}) \quad (2)$$

where

$$\eta_{\mathrm{DT}} = \eta_{\mathrm{M}}\eta_{\mathrm{TC}}\eta_{\mathrm{FD}} \quad (3)$$

On the urban schedule, the cumulative FCS efficiency (η_{FCS}) is 60.5%, the cumulative drive train efficiency (η_{DT}) is 75% and the vehicle accessory losses (ξ_{acc}) are 7.5%; these combine to give a TTW efficiency of 41.9%. The three components of the drive train, traction-inverter motor (TIM), torque coupler (TC) and the final drive (FD), have efficiencies of 85.8% (η_{M}), 94% (η_{TC}) and 93% (η_{FD}), respectively.

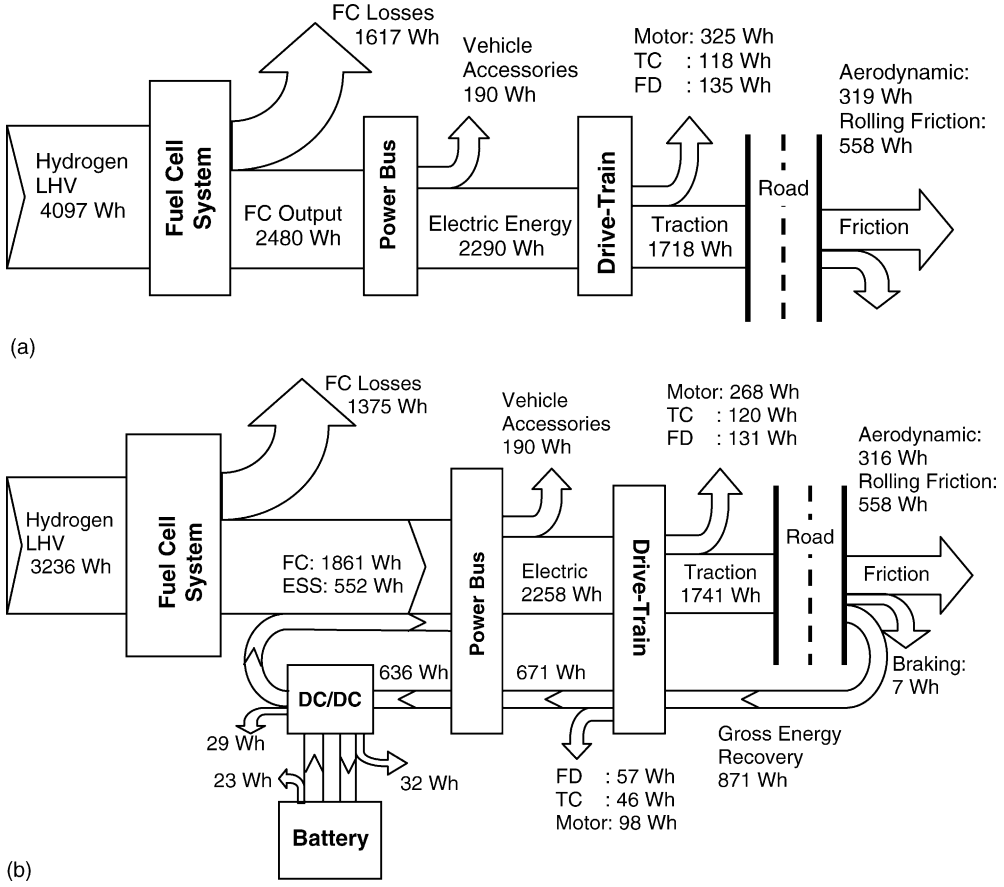

Fig. 10. Energy flow within the components of FCEV and FCHEV for FUDS: (a) stand-alone FCEV; (b) FCHEV with 65 kWe FCS and 55 kWe ESS.

For the hybrid power train, the TTW efficiency is given by the following product:

$$\eta_{\mathrm{TTW}} = \frac{\eta_{\mathrm{FCS}}\eta_{\mathrm{DT}}(1-\xi_{\mathrm{acc}})}{1-\beta} \tag{4}$$

where β is the fraction of the electric energy provided to the power bus by regenerative braking. It can be shown that β is related to the fraction of the traction energy that is involved in braking (f_{B}), the fraction of the braking energy that is dissipated through mechanical braking (ξ_{MB}), the efficiency of the drive train in regenerative braking mode ($\eta^{\mathrm{G}}_{\mathrm{DT}}$), the fraction of the regenerated power that is directly fed to the accessory load (ξ_{net}), and the round-trip efficiency (η_{s}) of the energy storage system including the dc/dc converter between the ESS and the traction motor:

$$\beta = \eta^{\mathrm{G}}_{\mathrm{DT}} f_{\mathrm{B}}(1-\xi_{\mathrm{MB}})\eta_{\mathrm{DT}}(1-\xi_{\mathrm{acc}})(\xi_{\mathrm{net}} + (1-\xi_{\mathrm{net}})\eta_{\mathrm{s}}) \tag{5}$$

where

$$\eta_{\mathrm{s}} = \eta^{\mathrm{C}}_{\mathrm{ESS}}\eta^{\mathrm{D/C}}_{\mathrm{ESS}}\eta^{\mathrm{C}}_{\mathrm{DC}}\eta^{\mathrm{D/C}}_{\mathrm{DC}} \tag{6}$$

$$\eta^{\mathrm{G}}_{\mathrm{DT}} = \eta_{\mathrm{G}}\eta_{\mathrm{TC}}\eta_{\mathrm{FD}} \tag{7}$$

Fig. 10b indicates that the hybrid power train with a 65 kWe FCS and a 55 kWe ESS has a TTW efficiency of 53.5% on the urban schedule. For this power train, the FCS efficiency on FUDS is 57.5%, the drive train efficiency for traction is 77.1%, and the vehicle accessory loss is 7.8%. About 23.9% (β) of the electric energy to the power bus is supplied by regenerative braking. The braking energy represents about 50% (f_{B}) of the traction energy for the urban schedule, nearly 1% of which is dissipated in the mechanical brakes (ξ_{MB}). The drive train converts 77% ($\eta^{\mathrm{G}}_{\mathrm{DT}}$) of the recovered braking energy into electrical energy; the calculated generator efficiency (η_{G}) is 87.2%. We estimate that about 10% of the electrical energy is lost in the dc/dc converter (i.e., $\eta^{\mathrm{C}}_{\mathrm{DC}}\eta^{\mathrm{D/C}}_{\mathrm{DC}} = 0.9$) and 4% is lost in the charge (subscript C) and discharge (subscript D/C) cycles of the ESS (i.e., $\eta^{\mathrm{C}}_{\mathrm{ESS}}\eta^{\mathrm{D/C}}_{\mathrm{ESS}} = 0.95$) so that the round-trip efficiency of the ESS and the dc/dc converter is 86.7% (η_{s}).

3.1. Effect of drive cycles

Fig. 11 illustrates the effect of drive cycles on the simulated fuel economy of FCEV and FCHEV. The results are given on the basis of mpgge and have not been adjusted for real world driving experiences. As mentioned earlier, the fuel economy increases by about 3% on FHDS and by 27% on FUDS as the FCS is downsized from 120 kWe (DOH = 0) to 65 kWe (DOH = 0.46). On US06 drive schedule, the maximum improvement in fuel economy is about 7%. On J1015

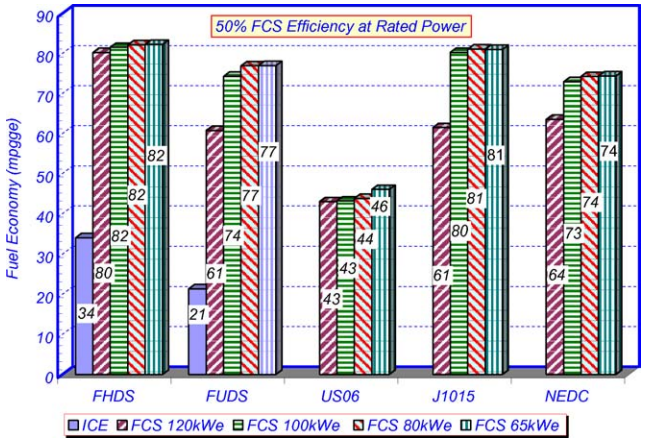

Fig. 11. Effect of drive cycles on fuel economy.

drive schedule and NEDC, the fuel economy improves with DOH; the maximum improvement is about 32% on J1015 and 17% on NEDC.

One parameter that determines the potential improvement in fuel economy with hybridization is the fraction of the traction energy that is involved in braking in a given drive cycle. The potential improvement is small in FHDS because the braking energy is only 13% of the traction energy and is large in FUDS and the J1015 cycle in which it is 50% and 53%, respectively. The braking energy fraction is 34% in US06 driving schedule and 35% in NEDC.

The fraction of the braking energy that is actually recovered depends on the size of the ESS and the braking power involved. Fig. 12 shows the recoverable and recovered braking energy fractions for different drive cycles as a function of DOH. The recoverable fraction of the braking energy is less than 85% on US06 drive schedule because it involves hard braking but can be more than 99% on J1015 drive schedule that has soft braking. Also, the recoverable and recovered fractions of the braking energy improve only slightly on J1015 drive schedule as the ESS peak power is raised from 20 to 55 kWe but nearly double on the US06 drive schedule.

Fig. 12 also shows the effect of drive cycles and DOH on cumulative FCS efficiency. Of the five cycles considered in this study, FHDS and J1015 schedule are the least aggressive as they have the lowest average power demand and, therefore, have the highest cumulative FCS efficiency. On the other hand, US06 schedule is the most aggressive as it has the highest power demand and, therefore, the lowest cumulative FCS efficiency. As noted earlier, the drive-cycle efficiency of FCS degrades as the FCS is downsized. Fig. 12 indicates that the more aggressive the drive cycle, the higher the degradation in cumulative efficiency of FCS as it is downsized. Thus, as the FCS is downsized from 120 to 65 kWe, the cumulative efficiency of FCS decreases by about 2% points on the less aggressive FHDS and J1015 schedule, 3% points on FUDS and NEDC, and >4% points on the more aggressive US06 schedule.

3.2. Effect of FCS efficiency

Fig. 13 presents the adjusted fuel economy of FCEV propelled by FCS with 40% efficiency at rated power. The stack in these FCS operates at a cell voltage of 575 mV at the rated power point (versus 690 mV for a 50%-efficient FCS at rated power) and has a specific power of 1200 W kg^{-1} (versus 780 W kg^{-1} for 50%-efficient FCS at rated power). A comparison with the results in Fig. 8 indicates that the effect of reducing the FCS efficiency at rated power (from 50% to 40%) on vehicle fuel economy is small both on FHDS and FUDS (<4 mpgge, <4.5%). On FUDS, the decrease in fuel economy depends on the FCS rated power (which depends on DOH): the larger the rated power (i.e., the lower the DOH), the smaller the effect of FCS efficiency at rated power on the fuel economy.

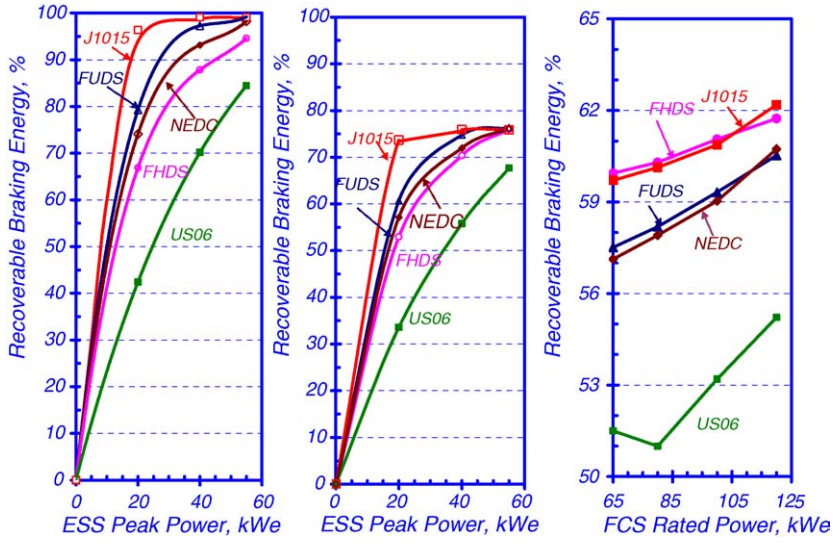

Fig. 12. Effect of drive cycles on recoverable braking energy and FCS efficiency.

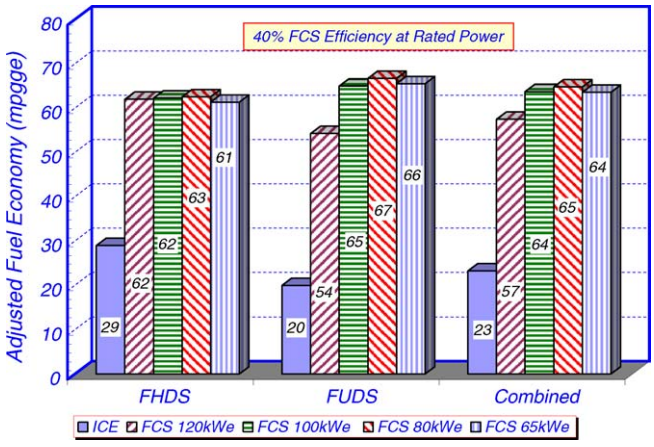

Fig. 13. Fuel economy with 40%-efficient FCS at rated power.

On the combined cycle, the difference between the fuel economies with 40% and 50% efficient FCS at rated power is <0.5 mpgge for the FCEV but >3.5 mpgge (∼5%) for the FCHEV with 46% DOH. Thus, whereas the advantage of selecting a 50%-efficient over a 40%-efficient FCS at rated power is small for a FCEV (especially if the cost is taken into account), it can be significant for a FCHEV and must be carefully evaluated.

3.3. Effect of cold start

Three of the five cycles analyzed in this study involve cold start after overnight parking. For these cycles, Table 4 summarizes the differences in simulated fuel economies between cold start of FCS at 20 °C and warm start of FCS at 80 °C. The penalty in fuel economy due to cold start is smaller on the less aggressive FUDS and NEDC (1–4.5%) than on the more aggressive US06 schedule (4.5–8%). The penalty is smaller for the stand-alone FCEV than for the FCHEV. However, it takes longer to heat the larger stack for the FCEV than for the smaller stack for the FCHEV. Over a single drive cycle (FUDS), we calculate that the stack temperature rises to 45 °C for the 120 kWe FCS and 52 °C for the 65 kWe FCS. Thus, if the vehicle is driven over multiple cycles, the total penalty in fuel economy is likely to be larger for the FCEV than for the FCHEV.

3.4. Effect of target SOC

With a given ESS, the fuel economy of the hybrid vehicle can be raised on demand by lowering the target SOC and sacrificing the performance (i.e., the stored energy). We ran simulations to evaluate the effect of target SOC on the fuel economy of FCHEV on US06—the most aggressive drive cycle considered in this study and for which the fuel economy of the FCEV is 43 mpgge. Fig. 14 shows that by lowering the target SOC to 0.55 from 0.65 the recoverable fraction of the braking energy increases to 92% from 84% with the 55 kWe ESS, to 80% from 70% with the 50 kWe ESS, and to 51% from 42% with the 20 kWe ESS. The resulting improvement in fuel economy is 1, 1.5 and 0.7 mpgge in hybrids with 55, 40 and 20 kWe ESS, respectively. The increase in fuel economy is obviously realized at the expense of the available energy: lowering the target SOC to 0.6 from 0.65 causes the energy available from the lithium-ion battery between SOC_{min} and the target SOC at C_1/1 rate to decrease by 14% and by 29% if the target SOC is lowered to 0.55.

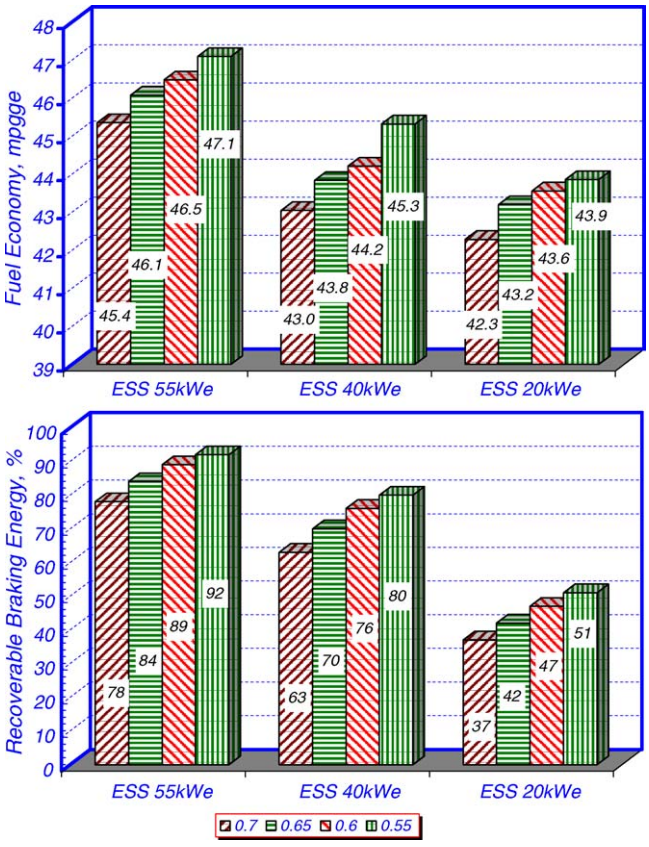

Fig. 14. Effect of target SOC on fuel economy on US06 drive schedule.

Table 4
Effect of cold start on fuel economy

Start-up	FUDS			US06			NEDC		
	Warm	Cold	Penalty	Warm	Cold	Penalty	Warm	Cold	Penalty
FCS-120 kWe	61.4	60.8	−1.0	45.1	43.0	−4.5	64.6	63.6	−1.6
FCS-100 kWe	75.1	74.3	−1.0	46.5	43.2	−7.0	74.0	72.7	−1.7
FCS-80 kWe	80.1	76.9	−4.0	47.8	43.8	−8.2	76.9	74.3	−3.5
FCS-65 kWe	80.6	77.0	−4.5	49.9	46.1	−7.7	77.6	74.4	−4.1

Table 5
Summary of simulation results

Platform	FCEV: 120 kWe FCS					FCHEV-1: 100 kWe FCS and 20 kWe ESS				
	FHDS[a]	FUDS	US06	J1015	NEDC	FHDS	FUDS	USO6	J1015	NEDC
FCS efficiency, η_{FCS} (%)	61.7	60.5	55.2	62.2	60.7	61.1	59.3	53.2	60.9	59.0
Drive train efficiency, η_{DT} (%)	80.5	74.5	79.7	74.3	75.6	80.1	77.6	79.1	77.3	78.6
Regenerative energy, β (%)	0.0	0.0	0.0	0.0	0.0	4.5	18.7	6.4	23.3	12.7
TTW efficiency, η_{TTW} (%)	47.6	41.5	42.7	41.2	42.4	49.1	52.0	43.8	54.7	49.0
Traction enemy (Wh)	2081	1720	2683	581	1533	2091	1753	2738	592	1550
Fuel economy (mpgge)	80.2	60.3	43.0	61.5	63.5	81.6	74.3	43.2	80.3	72.9
	FCHEV-2: 80 kWe FCS and 40 kWe ESS					FCHEV-3: 65 kWe FCS and 65 kWe ESS				
FCS efficiency, η_{FCS} (%)	60.3	58.2	51.2	60.1	57.9	59.9	57.5	51.5	59.7	57.1
Drive train efficiency, η_{DT} (%)	80.1	77.0	80.2	77.3	78.2	80.1	77.1	80.2	77.3	78.2
Regenerative energy, β (%)	6.2	23.3	11.2	24.6	16.1	6.7	24.0	14.8	24.8	17.1
TTW efficiency, η_{TTW} (%)	49.3	53.7	45.1	54.9	49.7	49.3	53.5	47.3	54.6	49.7
Traction enemy (Wh)	2084	1747	2733	589	1546	2073	1739	2727	586	1540
Fuel economy (mpgge)	82.1	76.9	44.6	81.1	74.3	82.3	77.0	46.8	81.0	74.4

[a] Drive cycle.

4. Summary and conclusions

We have compared the fuel economy of a class of stand-alone and hybrid fuel-cell electric vehicles that have similar drivability and performance characteristics (top speed, acceleration and on-grade towing capability) as the reference ICEV on a common platform. For the five drive cycles analyzed in this work Table 5 compares the traction power demand, efficiency and fuel economy and leads to the following main conclusions:

- The potential gain in fuel economy with hybridization is higher for ICEV than for FCEV. On a hybrid platform the smaller ICE is more efficient than the larger ICE in a conventional vehicle. Although the FCS is more efficient than the ICE, its drive-cycle efficiency actually decreases if it is downsized for deployment on a hybrid platform.
- With FCEV the gain in fuel economy with hybridization comes from regenerative braking and therefore depends on drive cycles. The fraction of the traction energy that is expended on braking is 13% on FHDS, 34% on US06 schedule, 35% on NEDC, 50% on FUDS and 53% on J1015 schedule. If 100% of the braking energy was recoverable at the wheels the resulting maximum increase in the fuel economy of a FCEV would be 7% on FHDS, 20% on US06, 20% on NEDC, 30% on FUDS, and 31% on J1015 schedule.
- Our simulations of load-following FCS powered hybrid vehicles indicate that the fraction of the braking energy that is recoverable at the wheels can be up to 85% on US06 schedule, 94% on FHDS, 95% on NEDC and 99% on FUDS and J1015 schedule. For the different degrees of hybridization analyzed, regenerative braking provides the following fraction of the electric energy to the power bus: 4.5–6.7% on FHDS, 6.4–14.8% on US06 schedule, 12.7–17.1% on NEDC, 18.7–24% on FUDS and 23.3–24.8% on J1015 schedule. The overall TTW efficiencies for FCEV and FCHEV are 47.6% versus 49.3% on FHDS, 41.5% versus 53.5% on FUDS, 42.7% versus 47.3% on US06 schedule, 42.4% versus 49.7% on NEDC, and 41.2% versus 54.6% on J1015 schedule.
- The estimated increase in fuel economy of a FCEV by hybridizing it with a Li-ion battery pack is 3% on FHDS, 7% on the aggressive US06 drive schedule, 17% on NEDC, 27% on the stop-and-go FUDS, and 32% on J1015 drive schedule.
- On the aggressive US06 schedule the fuel economy can be further increased on demand by 3.5% by sacrificing some of its performance in terms of the amount of stored energy that can be withdrawn from the battery before recharging.
- On the combined FUDS and FHDS used in EPA tests the simulated fuel economy of the FCEV is 2.5 times the published fuel economy of the ICEV on the same platform. With FCHEV the fuel economy multiplier can further increase to 2.9.

Acknowledgements

This work was supported by the U.S. Department of Energy's Office of Energy Efficiency and Renewable Energy, Office of Hydrogen, Fuel Cells, and Infrastructure Technologies and the Office of FreedomCAR and Vehicle Technologies.

References

[1] Well-to-Wheel Energy Use and Greenhouse Gas Emissions of Advanced Fuel/Vehicle Systems—North American Analysis, vol. 2, General Motors Corporation, 2001.
[2] M.A. Weiss, J.B. Haywood, A. Schafer, V.K. Natarajan, Comparative Assessment of Fuel Cell Cars, Publication No. LFEE 2003-001 RP, Massachusetts Institute of Technology, Laboratory for Energy and the Environment, 2003.

[3] Well-to-Wheels Analysis of Future Automotive Fuels and Powertrains in the European Context—Tank-to-Wheels Report, version 1, Concawe, EUCAR and European Commission Directorate-General Joint Research Centre, 2003.
[4] R.K. Ahluwalia, X. Wang, A. Rousseau, R. Kumar, Fuel economy of hydrogen fuel cell vehicles, J. Power Sources 130 (2003) 192–201.
[5] R.K. Ahluwalia, X. Wang, Direct hydrogen fuel cell systems for hybrid vehicles, J. Power Sources 139 (2005) 152–164.
[6] H.K. Geyer, R.K. Ahluwalia, GCtool for Fuel Cell Systems Design and Analysis: User Documentation, Argonne National Laboratory Report ANL-98/8, 1998.
[7] A. Rousseau, P. Pasquier, Validation Process of a System Analysis Model: PSAT, in: Proceedings of the SAE World Conference, SAE Paper 01-P183, Detroit, MI, March 5–8, 2001.
[8] UQM Technologies Traction Drive System, http://www.uqm.com, January 30, 2001.